MODELLING TYRE-ROAD CONTACT STRESSES IN PAVEMENT DESIGN AND ANALYSIS

J W MAINA, M DE BEER, and Y VAN RENSBURG

CSIR Built Environment, Bldg 2C, P O Box 395, Pretoria, 0001, South Africa
Tel: 012 841 3956; Email: JMaina@csir.co.za

ABSTRACT

Growing traffic volumes, increasing construction and maintenance costs continually drive for more innovative approaches and methodologies towards sustainable road infrastructure. At the current price levels of around R6000 per metric tonne, bitumen, as a "raw" product, is by far the most costly element in flexible pavements, for example compared to Crushed stone, which is at approximately R170 per metric tonne. Since the asphalt layer or relatively thin bituminous seal acts as the stress barrier between rolling tyres and the road structure it needs to be durable so as to withstand current traffic loading and hence contact stresses, given the environmental forces also acting on it. For road infrastructure to perform as expected, it is important to optimize road pavement design, especially close to the surface of the pavement requiring accurate modelling of tyre-road contact stresses.

The aim of this paper is to demonstrate modern ways to idealise tyre-road interaction based on Stress-In-Motion (SIM) results, in particular the way in which numerical analyses are used (and developed) to address non-uniformly distributed tyre contact stresses on the surface of the pavements. A tyre model is demonstrated whereby the SIM measured contact stress distribution is idealised with a multitude of circular and rectangular shapes, mimicking the non-uniform characteristics of the contact stresses inside the tyre contact patch. An example, in terms of pavement layer life and strain energy of distortion, is given highlighting the effects of different tyre-road models on a typical flexible road structure, compared to the traditional circular shape model of a single uniformly distributed contact stress (1D).

1 INTRODUCTION

By supporting movement of people and goods, access to education and training, employment and health care, a sound road network plays a key role in socio-economic development of a country. The South African Pavement Design Method (SAPDM) is in the final stages of its revision. SAPDM is expected to respond well to the current reality in the growth of both passenger and freight traffic as a result of increased economic activities. Forming part of this revision is the need for advanced numerical modelling of tyre-road contact stresses. The modelling will provide a better understanding of the impact of increased loading on performance of South African transport infrastructure, specifically roads and its associated protected surfacings.

Tyres form an essential interface between vehicles and road pavement surfaces as they are the only parts of a vehicle that are in contact with the road. Tyres are used to transmit the vehicle loading to the road surface through a very small contact area, generally called the 'contact patch' or 'tyre footprint'. By using fewer tyres and carrying heavier cargo, modern trucks are exerting much higher contact stresses on the road surface than their predecessors. A good understanding and the capability to model tyre-road contact stresses are, therefore, important for better road pavement designs, and hence good performance of roads.

Numerous research works were performed in the past in order to find solutions when load contact patch acting on the surface of a semi-infinite medium is considered to be circular (Poulos and Davis, 1974). Two approaches can be utilized to solve such problems. The first method uses Boussinesq functions and the second method uses Hankel transforms as formulated by Terazawa or Sneddon (Muki, 1956). While it is required to perform double Fourier integrals for methods using the first approach, the merit in using the second approach is on the requirement to solve only one integral (Maina and Matsui, 2004).

On the other hand, when the load contact patch considered is rectangular in shape, symmetry in the axial direction is lost and thus the use of a cylindrical coordinate system becomes complicated as the application of Hankel Transforms may not be appropriate. Thompson *et al.* (1987) presented the solution for a general shape uniform load acting on the surface of a semi-infinite medium. However, extending this solution to a multi-layered elastic system is difficult and the Finite Element Method (FEM) is often utilized because of its flexibility in handling complex boundary value problems, including irregular loading conditions such as rectangular loads (Dong *et al.,* 2002, Mulungye *et al.,* 2005, Nishizawa *et al.,* 2003). Rectangular loads used in FEM may very closely simulate the actual shape of the tyre contact patch as well as the distributed load. However, since FEM is an approximate method, its accuracy is highly dependent on the mesh generation and user experience is very important. Further, FEM is not good at computing stresses accurately in the neighbourhood of inter-element boundaries as it assumes displacement fields within an element by nodal displacements and assumed pre-defined shape functions.

Solutions using these two approaches in terms of pavement layer lives as well as strain energy of distortion (SED) as defined by Timoshenko and Goodier (1951) – used here as an indicator for potential of pavement failure – are presented and compared in this paper. Comparison between responses from circular and rectangular load patches may be of high interest to pavement engineers as it will show whether, if at all, these two methods give significantly different results.

2 TYRE-ROAD CONTACT STRESS MEASUREMENTS

2.1 Stress-In-Motion (SIM) Technology

During the 1990s a rigid flatbed device with a textured surface was successfully developed and used to measure the tire-pavement contact stresses of a range of pneumatic truck tires. The single pad of this device, referred to as the SIM device (De Beer, 2008). The SIM device was developed mainly for the measurement of slow-moving pneumatic truck tires (speed approx. 5 km/h). A single SIM pad consists of 21 instrumented conically shaped hollow cylindrical pins in a linear configuration across the SIM device. The circular surface contact area of a single pin is approximately 73.9 mm^2 (diameter of 9.7 mm) at a fixed lateral resolution of 17 mm c/c (See also De Beer *et al.,* 2012).

The SIM measurements can now be used as input data for mechanistic-empirical (ME) pavement modeling and analysis by General Analysis for Multi-layered Elastic Systems (GAMES) software (also referred to as multi-layer linear elastic (MLLE) analysis) considering the load shape to be either circular or rectangular. Results from this software may be used for pavement damage studies in terms of predicting potential for fatigue failure (cracking) or permanent deformation (rutting), as reported by De Beer *et al.,* 2012.

2.2 Idealization of tyre-contact stresses for road pavement analysis

In Figure 1 and Figure 2, schematics are shown defining "Conventional" and "Pin" areas that are used for the tyre-pavement contact stresses. These two circular areas are defined for purposes of mechanistic-empirical analysis The "Conventional" area refers to a tyre contact patch represented by a single circle with diameter of 221.3 mm whereas "Pin" to a tyre contact patch represented by 206 multiple circles with diameter of 9.7 mm each.
Another numerical approach that is also considered in this paper assumes the load patch contact shapes to be rectangular in shape as shown in Figure 3 and Figure 4. In this regard, and for consistency in the comparison of results, a representation of rectangular "Pin" area referred to a square area of 8.6 mm. An additional rectangular area (also known as texture neutral *(TN)*) was also considered with blocks of rectangular shaped (14.7224 mm x 17 mm) load idealization touching each other and covering the entire measured tyre contact patch.

2.3 Tyre Contact-Stress Models

For purposes of pavement analysis, five tyre-pavement contact stress models were considered in this paper, following on from similar research by De Beer *et al.,* 2012. Only contact stresses in the vertical direction (1D) were used in the analysis of this paper:

Contact-Stress Model 1: Representing data for single load on a circular area with load radius r of 110.65 mm. This model represents a conventional 20 kN tyre load at 520 kPa inflation pressure. See Figure 1.

Contact-Stress Model 2: Representing data for multiple of 206 smaller circular disks (i.e. *pin area*) with a radius of 4.85 mm. This model represents the circular area of SIM pin heads. See Figure 2.

Contact-Stress Model 3: Representing data for multiple of 206 smaller square disks (area equivalent to the *pin area of Model 2*) of 8.6 mm x 8.6 mm. This model represents the area of SIM pin heads in a rectangular form. See Figure 3.

Contact-Stress Model 4: Representing data for multiple of 206 larger rectangular disks (defined as the effective area and referred to as a "*Texture Neutral", (TN)* of size 14.7224 mm x 17.0 mm). This model represents a fully loaded tyre patch with the rectangles touching each other. See Figure 4.

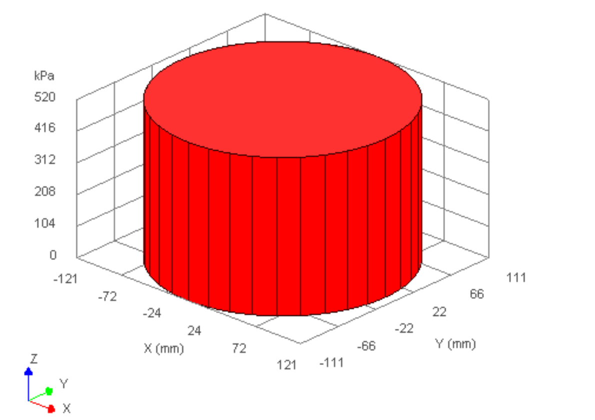

Figure 1. Model 1 - Contact Stress – Conventional circular load with radius r = 110.65 mm.

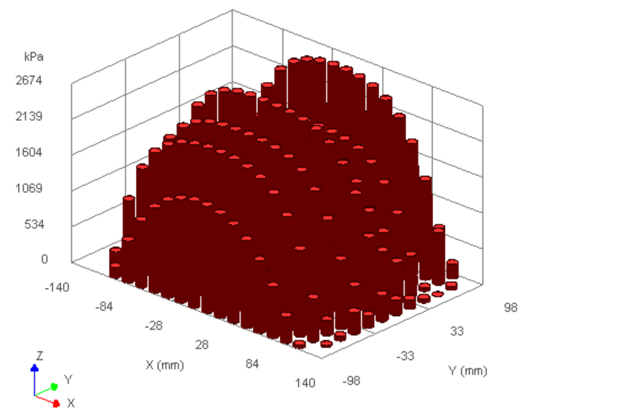

Figure 2. Model 2 - 206 Multiple circular pin area with r = 4.85 mm.

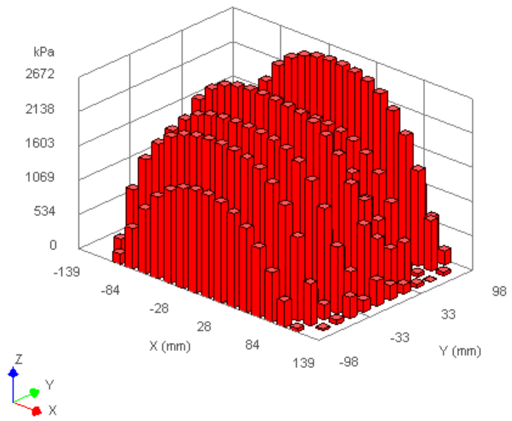

Figure 3. Model 3 - Contact Stress - Rectangular Pin area: 8.6 mm x 8.6 mm.

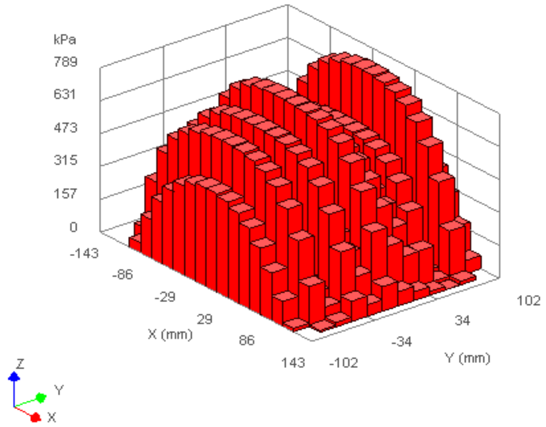

Figure 4. Model 4 - Contact Stress - Rectangular Texture Neutral area (14.7224 mm x 17 mm).

3 PAVEMENT ANALYSIS

3.1 Pavement structure

In order to compare results from circular and rectangular loads and quantify their differences as well as their impact in a pavement design, a pavement structure shown in Figure 5 was considered. This is a 5-layer flexible road pavement structure whereby elastic modulus, Poisson's ratio and layer thickness values were estimated based on recommendations by Theyse *et al.,* (1996).

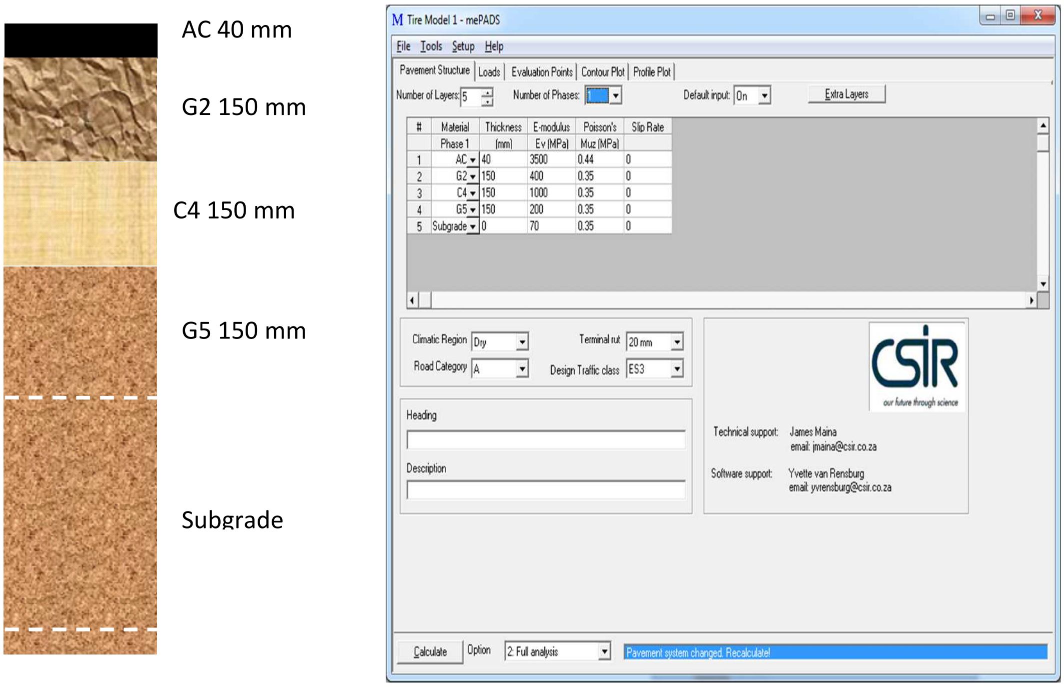

Figure 5. 5 – Layer Pavement and material definition for multi-layer linear elastic (MLLE) analysis

Notes on the Material Codes Used in Figure 5

AC: asphalt surfacing layer; G2: Graded crushed stone; C4: lightly cemented natural gravel; G5: Natural gravel selected layer; Subgrade: In-situ subgrade layer.

3.2 Theoretical formulation for circular loads

As mentioned in section 2, only vertical load is considered in this study. For the case of a circular load where the vertical load is applied at the surface and is uniformly distributed over a circle of radius *a*, the problem is axi-symmetric. It is, therefore, convenient to use a cylindrical coordinate system (r, z). Further, the pavement is assumed to be composed of *n* layers parallel to each other and the bottom layer (n^{th} layer) is semi-infinite. If u_r and u_z are displacement components in the *r*- and *z*-directions, respectively, the governing equations can be written as,

$$\nabla^2 u_r + \frac{1}{1-2\nu}\frac{\partial}{\partial r}\left(\frac{\partial u_r}{\partial r} + \frac{u_r}{r} + \frac{\partial u_z}{\partial z}\right) - \frac{u_r}{r^2} = 0 \quad (1)$$

$$\nabla^2 u_z + \frac{1}{1-2\nu}\frac{\partial}{\partial z}\left(\frac{\partial u_z}{\partial z} + \frac{u_r}{r} + \frac{\partial u_r}{\partial r}\right) = 0 \quad (2)$$

where, ν is a Poisson's ratio and ∇^2 is the Laplace operator given as

$$\nabla^2 = \frac{\partial^2}{\partial r^2} + \frac{1}{r}\frac{\partial}{\partial r} + \frac{\partial^2}{\partial z^2} \quad (3)$$

Boundary conditions can be given as shown in Eqs. (4), since the surface loading is uniformly distributed over a circular area.

When $r \le a$

$$\sigma_z(r,0) = -p\,, \quad \tau_{rz}(r,0) = 0 \quad (4a)$$

and when $r > a$

$$\sigma_z(r,0) = \tau_{rz}(r,0) = 0 \quad (4b)$$

If one solves Eqs. (1) and (2) taking into account boundary conditions presented in Eq. (4), axi-symmetric solutions can be obtained.

3.3 Theoretical formulation for rectangular loads

In the analysis of rectangular loads, a system of rectangular Cartesian coordinates (*x, y, z*) is used. By assuming the body forces to be zero, equilibrium equations may be written as a function of displacement as follows:

$$\mu\left(\frac{\partial^2}{\partial x^2} + \frac{\partial^2}{\partial y^2} + \frac{\partial^2}{\partial z^2}\right)u + (\lambda + \mu)\frac{\partial}{\partial x}\left(\frac{\partial u}{\partial x} + \frac{\partial v}{\partial y} + \frac{\partial w}{\partial z}\right) = 0 \quad (5a)$$

$$\mu\left(\frac{\partial^2}{\partial x^2}+\frac{\partial^2}{\partial y^2}+\frac{\partial^2}{\partial z^2}\right)v+(\lambda+\mu)\frac{\partial}{\partial y}\left(\frac{\partial u}{\partial x}+\frac{\partial v}{\partial y}+\frac{\partial w}{\partial z}\right)=0 \qquad (5b)$$

$$\mu\left(\frac{\partial^2}{\partial x^2}+\frac{\partial^2}{\partial y^2}+\frac{\partial^2}{\partial z^2}\right)w+(\lambda+\mu)\frac{\partial}{\partial z}\left(\frac{\partial u}{\partial x}+\frac{\partial v}{\partial y}+\frac{\partial w}{\partial z}\right)=0 \qquad (5c)$$

where σ_x, σ_y, σ_z, τ_{xy}, τ_{xz}, and τ_{yz} are stresses in an infinitesimal element. Strain-displacement relationship may be represented as follows:

$$\lambda=\frac{E\nu}{(1+\nu)(1-2\nu)};\ \mu=\frac{E}{2(1+\nu)} \qquad (6a)$$

$$\varepsilon_x=\frac{\partial u}{\partial x},\ \varepsilon_y=\frac{\partial v}{\partial y},\ \varepsilon_z=\frac{\partial w}{\partial z},\ \gamma_{xy}=\frac{\partial v}{\partial x}+\frac{\partial u}{\partial y},\ \gamma_{xz}=\frac{\partial u}{\partial z}+\frac{\partial w}{\partial x},\ \gamma_{yz}=\frac{\partial w}{\partial y}+\frac{\partial v}{\partial z} \qquad (6b)$$

where E and ν are elastic modulus and Poisson's ratio of the layer material whereas u, v, and w are displacements in the directions of x-, y-, and z-axes. Furthermore, ε_x, ε_y, and ε_z are normal strains corresponding to normal stresses σ_x, σ_y, and σ_z, while γ_{xy}, γ_{xz}, and γ_{yz} are shear strains corresponding to shear stresses τ_{xy}, τ_{xz}, and τ_{yz}. Boundary conditions for rectangular loads acting on a surface of a semi-infinite medium may be represented as shown below:

when $x \le |a|$ and $y \le |b|$ then;

$$\sigma_z(x,y,0)=-p_z,\quad \tau_{xz}(x,y,0)=-p_x,\ \tau_{yz}(x,y,0)=-p_y \qquad (7a)$$

when $x > |a|$ and $y > |b|$ then;

$$\sigma_z(x,y,0)=\tau_{xz}(x,y,0)=\tau_{yz}(x,y,0)=0 \qquad (7b)$$

where a and b are length and width of the load area, respectively. If one solves Eqs. (5), taking into account boundary conditions presented in Eq. (7), rectangular solutions can be obtained.

3.4 Estimating pavement bearing capacity (Theyse et al. 1996)

Individual layer life in terms of permanent deformation and/or cracking together with occurrence of crushing in cemented layers (when present) are usually used to predict ultimate pavement bearing capacity also known as pavement life. Pavement layers are constructed using different materials and these materials exhibit unique modes of failure. The failure mode for each individual layer is dependent on a particular critical resilient response parameter. The failure mechanism of each material is determined first in a laboratory setup, where the material is tested until failure. After that, the relationship between critical resilient response parameter and number of load repetition through accelerated pavement testing or long term pavement performance studies is determined to establish what is known as the transfer function. This means using (transferring) the material failure in the laboratory to predict failure of the same material out in the field.

According to Maree and Feeme (1981), granular base materials fail by shear deformation (densification) and the critical resilient response parameters are the major and minor principal stresses usually calculated at the mid-point of a granular layer. Prediction of shear deformation in lower unbound layers, e.g. subgrade is based on vertical strain. On the other hand, cemented materials fail either by cracking or crushing and the critical parameter for cracking is the maximum tensile strain at the bottom or in the layer and critical parameter for crushing is the vertical compressive stress on top of the cemented layer (De Beer, 1990). Two transfer functions are provided for crushing, namely crush initiation with roughly 2 mm deformation on top of the cemented layer and advanced crushing with 10 mm deformation and extensive breakdown of the cemented material. Lastly, asphalt materials fail by fatigue cracking and the critical resilient response parameter is the tensile strain at the bottom or in the asphalt layer. Transfer functions are provided for continuously graded or gap graded thin surfacing layers (< 50 mm thick) and asphalt base layers (> 75 mm thick).

The critical parameters and points vary for different material types as summarized below:

- Asphalt layers. The elastic horizontal tensile strain at the bottom of the layer controls the fatigue life of the layer.
- Cemented layers. The elastic horizontal tensile strain at the bottom of the layer controls the effective fatigue life of the layer, while the elastic vertical compressive stress at the top of the layer controls the crushing life.
- Granular layers. The major and minor principal stresses at the middle of the layer controls the shear potential of the layer.
- Soil (Subgrade) layers. The elastic vertical compressive strain on the top of the layer controls the rutting life of the subgrade.

4 ANALYSIS RESULTS

The objectives of this paper are two-fold. The first objective, as is always true for the case involving development of numerical tools, is to demonstrate the accuracy of the algorithms used by way of comparison of measured contact stresses with computed values. The second objective is to quantify the effect of different tyre models on the prediction of pavement bearing capacity.

4.1 Validating the algorithms used

The best way to validate accuracy and reliability of the algorithms used is to compare the input contact stresses with output values as shown in Figure 6 to Figure 9. These figures show an excellent agreement between measured contact stresses and computed normal stresses at the surface of the pavement system. In all the four tyre-pavement contact stress models, results were almost 100% of the input values.

It took on average about one and a half hours on a workstation machine (12 GB RAM, 6 Intel® Xeon® CPUs W3680 @ 3.33GHz) to run analysis for rectangular loads and 2 minutes to analyse circular loads. The reason for the difference in computation time is that in the analysis of rectangular loading double integration is performed (x-y domain) whereas a single integration is required for the case of circular loading (r domain).

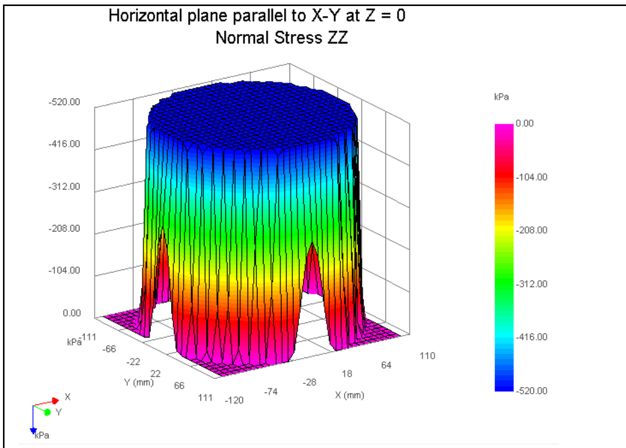

Figure 6. Vertical Stress – Conventional circular area

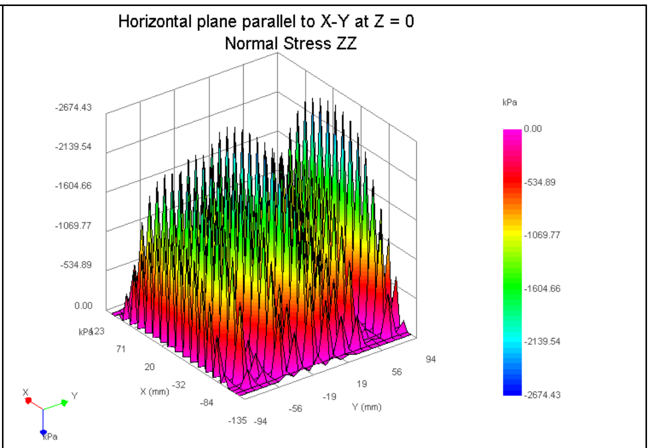

Figure 7. Vertical Stress - Circular Pin area

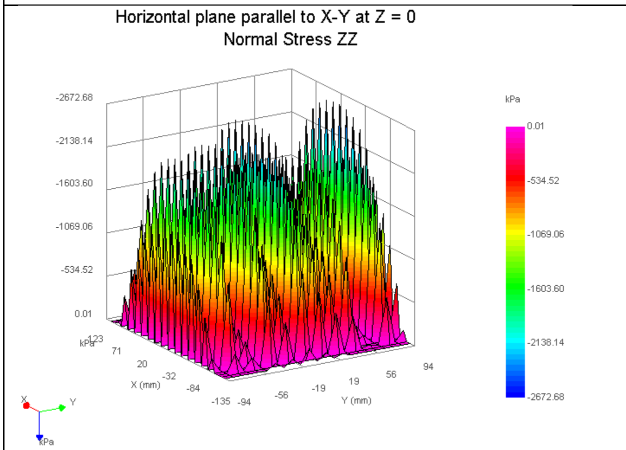

Figure 8. Vertical Stress - Rectangular Pin area

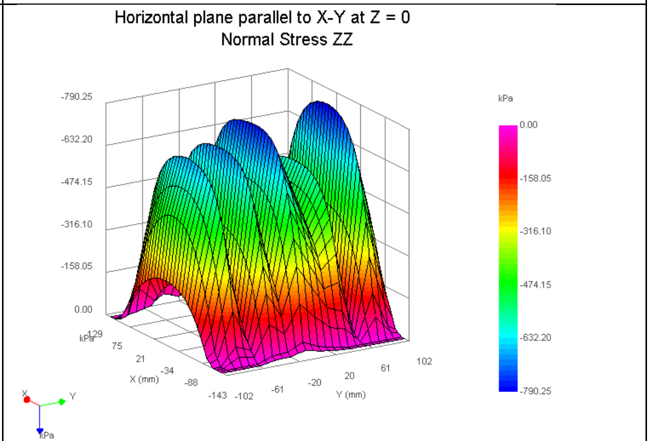

Figure 9. Vertical Stress - Rectangular Texture Neutral area

[redacted]**Table 1. Summary of the Asphalt layer bearing capacities and SED values relative to Model 1.**

Tyre Model	Input Max Vertical Stress (kPa)	Output Max Vertical Stress (kPa)	Diff. (%)	AC Fatigue Life (10^6)	SED (Nm/m^3)	Percentage Relative to Model 1	
						AC Fatigue Life	SED
1	520	520	0.00	2.37	156.63	100.00	100.00
2	2674	2674	0.00	0.89	195.59	37.55	124.87
3	2672	2673	-0.04	0.72	207.62	30.38	132.55
4	789	790	-0.13	1.23	178.09	51.90	113.70

SED = Strain Energy of Distortion in Nm/m^3. AC = Continuously graded asphalt surfacing layer.

Furthermore, Table 1 shows estimation of pavement bearing capacity for the asphalt layer, in terms of fatigue life and strain energy of distortion (SED), right under the centre of the load (x = 0 mm, y = 0 mm, z = 40 mm). Tyre model 1 was used as a reference point and results from other models were compared against it as shown in the two right hand columns in Table 1. The fatigue life values are valid for the load conditions specified in this study, which were 1 to 3 million equivalent single axle loads. Further, the analysis was done according to 95% design reliability associated with Road Category A (Theyse, *et al.,* 1996). What is interesting to note from the results shown in Table 1 is that, although fatigue life is determined through the use of transfer functions whereas SED is mechanistic based, they all show that the conventional tyre patch (Model 1) is less damaging to the pavement structure and the tyre contact stress represented by rectangular pin area (Model 3) appears to be more damaging followed by circular pin area (Model 2). The Model 4, which represents the effective area of the tyre-contact patch appears to be less damaging as compared to the rectangular and circular pin areas. This lower damaging effect may be attributed to the fact that a relatively bigger contact area is considered resulting in lower contact stresses. Analysis results (not shown here) of the supporting layers in Figure 5 indicated very little differences and is mainly as a result of St. Venant's principle (Love, 1927), which holds for linear elastic methodologies - showing the different loading models only affect the zone close to surface.

It is also important to consider implications of the analysis results presented above. In most of the existing pavement design methods, tyre Model 1 is used to idealize tyre loading and contact stress distribution on the surface of a pavement structure. On the other hand, Models 2 to 4 represent the actual contact stress distributions as captured by the SIM device. What the results, through the fatigue life and SED, tell us is that relative to the conventional load, e.g. Model 3 will result in a pavement structure, which is under designed by up to 69% in terms of fatigue life associated with higher damage potential of 132% in terms of SED. The implication of which is a possibility of premature pavement failures when a design is done using the conventional tyre patch for mechanistic-empirical (ME) pavement modelling.

It is also important to note that although the above relative ranking agrees, the M-E result is not necessarily a good indication of actual life due to lack of calibration of asphalt transfer functions, considered to be conservative and may therefore be a reason why effect of relative lower capacities (potential risk of "under design" compared to more realistic models) have not been observed. The results in this paper do not mean all asphalt surfaces were previously under designed

5 CONCLUSIONS AND RECOMMENDATIONS

The paper presented the results of using circular and rectangular load shapes to predict pavement life. It should also be recognized that these analyses were only feasible with the availability of advanced numerical tools developed at the CSIR, which have made it possible to analyse contact stresses measured by a SIM device without the need of a simplified contact stress idealization. With these findings in mind, the following conclusions and recommendations are made:

- Conventional load patch (Model 1) resulted in the asphalt layer meeting the design specification;
- Rectangular pin area load patch (Models 3 & 4) appears to be more damaging for the asphalt layer followed by circular pin area. For these two models, the asphalt layer did not meet the design specification;
- Model 4 representing the effective tyre contact area also called Texture Neutral barely satisfied the design requirement as the contact stress level for this model was also low;
- Only vertical contact stress distributions were used in this study, i.e. 1D. However, since SIM device is capable of measuring 3D contact stress distributions, the advanced tools should be used to compare the effect of using 1D against 2D or 3D contact stress information in the design and analysis of pavements;
- Combination of strain-energy-of-distortion with fatigue/permanent deformation failures should be used to establish points of interest on top or within a pavement structure that has the highest possibility of failure – not demonstrated in this paper;

ACKNOWLEDGEMENT
The authors would like to acknowledge the CSIR for funding this study.

REFERENCES

De Beer, M. 1990. Aspects of the Design and Behaviour of Road Structures Incorporating Lightly Cementitious Layers. Ph D Thesis, Department of Civil Engineering, Faculty of Engineering, University of Pretoria, Pretoria, South Africa.

De Beer, M. 2008. Stress-In-Motion (SIM) – A New Tool for Road Infrastructure Protection. WIM Session 7: International Conference on Heavy Vehicles (HVParis2008), Paris/Marne-la-Vallée.

De Beer, M., Maina, J.W., van Rensburg, Y and Jan M. Greben., 2012. Toward Using Tire-Road Contact Stresses in Pavement Design and Analysis. Tire Science and Technology: October-December 2012, Vol. 40, No. 4, pp. 246-271.

Dong, Q., Matsui K. and Hachiya. Y. 2002. Three-Dimensional Finite Element Analysis of Airfield Pavement Subjected to Moving Wheel Loads. Journal of Pavement Engineering, JSCE, Vol. 7, pp.207-216.

Love, A.E.H. 1927. A treatise on the mathematical theory of elasticity. Cambridge University Press.

Maina, J. W. and Matsui K. 2004. Developing Software for Elastic Analysis of Pavement Structure Responses to Vertical and Horizontal Surface Loadings. Transportation Research Records, No. 1896, pp. 107-118.

Maree, J.H., and Freeme, C.R., 1981. The Mechanistic Design Method Used to Evaluate the Pavement Structures in the Catalogue of the Draft TRH4 1980. Technical Report.

Muki, R., 1956. Three Dimensional Problem of Elasticity for a Semi-Infinite Solid with a Tangential Load on its Surface. Transactions of the Japan Society of Mechanical Engineers, Vol.22, No.119, pp. 468-474.

Mulungye, R.M., Owende P.M.O., and Mellon K. 2005. Finite element modeling of flexible pavement on soft soil subgrades. Materials and Design, 28, pp.739-756.

Nishizawa, T., Murata Y. and Kokubu K. 2003. Dynamic Behaviors of Ultra Thin White Topping Structure under Traffic Loading. Journal of Japan Society of Civil Engineers, JSCE, No. 725, V-58, pp.183-195.

Poulos, H.G. and Davis E.H. 1974. Elastic Solutions for Soil and Rock mechanics. John Wiley and Sons, Inc., New York, NY.

Theyse, H.L., De Beer, M. and Rust, F.C. 1996. Overview of South African Mechanistic Pavement Design Method. Transportation Research Record, (1539), pp. 6-17.

Thompson, J.C., Lelievre, Beckie, R.D. and Negus, K.J. 1987. A Simple Procedure for Computation of Vertical Soil Stresses for Surface Region of Arbitrary Shape and Loading. Canadian Geotechnique Journal, Vol. 24, pp.143-145.

Timoshenko, S., and Goodier J., N., 1951. Theory of Elasticity. 2nd Edition, McGraw-Hill Book Company, Inc.